Control of Flexible Structures by Applied Thermal Gradients

Donald L. Edberg*
Jet Propulsion Laboratory, California Institute of Technology, Pasadena, California

Thermal, elastic, and feedback analyses are applied to the case of a beam with a distributed thermal actuator. The actuator is capable of producing a thermal gradient across the section of the beam. One candidate for such an actuator uses the Peltier effect, which appears in certain semiconductors. These devices act as heat pumps when a voltage is applied, causing a temperature gradient. It is shown that the thermal gradients can induce deflection in the beam. If the thermal gradients are applied in the proper sense to a vibrating beam, it is possible to increase the vibration damping exhibited by the structure. Experimental results are given for a cantilever beam, whose first vibrational mode damping ratio was increased from 0.81 to 7.4% with simple lead compensation.

Nomenclature

A = cross-sectional area of beam
b = beam width
C_{QV} = voltage to heat flow conversion constant
$C(s)$ = compensator dynamics
c = specific heat
d = separation of cap neutral axis from beam centroid
E = Young's modulus
H = Heaviside step function
G_s = sensor gain coefficient
g = acceleration of gravity at Earth's surface
h = depth of beam cap
I = bending moment of inertia
i = electric current
K = thermal conductivity
K_c = compensator gain
$\mathcal{L}\{\ \}$ = Laplace transform of $\{\ \}$
ℓ = length of beam
ℓ_a = thermal length of beam section near actuator
M_T = bending moment induced by applied thermal gradient
$m(x)$ = beam mass distribution per unit length
n_s = number of thermal actuators in series
Q = thermal flux applied to beam cap
R = electrical resistance of thermoelectric modules
S = area where heat is applied ($=b\ell_a$)
s = Laplace transform variable
T_{step} = temperature perturbation caused by step heat input $= T_{\text{actual}} - T_{\text{ref}}$
T = $\partial T_{\text{step}}/\partial t$
t = time coordinate
V = voltage
V_c = compensator voltage
V_s = sensor voltage
x = spanwise coordinate
x_1, x_2 = coordinates at beginning and end of actuator
x_s = sensor location
$w(x)$ = lateral beam deflection
z = vertical coordinate from beam neutral axis
$\hat{z}$ = distance from cap outside
α = coefficient of thermal expansion
β_n = $\kappa n^2\pi^2 t/h^2$
δ_{mn} = Krönecker delta function
ζ = damping ratio, $= c/c_r$
κ = $K/\rho c$ (thermal constant)
$\xi_n(t)$ = modal expansion time function
ρ = mass density
$\varphi_n(x)$ = mass-normalized mode shape
$\varphi_n'(x)$ = slope of mass-normalized mode shape
ω = circular frequency
$(\ )'$ = derivative of $(\ )$ with respect to argument

Received June 20, 1986; revision received Sept. 19, 1986.

*Member of Technical Staff, Applied Technologies Section.

I. Introduction

LARGE space structures planned for the future are expected to have very low natural frequencies. Their damping properties are not easily predicted, but it seems clear that in order for them to perform properly, some active means of increasing their energy dissipation is almost sure to be necessary. There is an immense literature on the subject of control of large space structures, much of it dealing with optimal location, control algorithms, and structural design. This paper will not deal with those issues, but will instead address the idea of a different method of damping augmentation.

The theoretical study of damping mechanisms has been going on for quite some time. The work by Zener[1] is a classic in the field. More recently, the work on thermoelastic damping has been enriched by Ashley[2] and Lee.[3] All of these give a general result that is important to the current work, which is that the *material* damping of an object is explained by the flow of heat caused by stress-induced thermal gradients. These thermal gradients arise from the nonuniform partial conversion of vibrational elastic energy into heat. Of course, a detailed description of these gradients depends on material properties and specimen geometry. The reader is referred to the previous references for further details.

A simple, qualitative description of this phenomenon is useful to the present analysis. As an example, consider a beam in bending vibration. As the beam deforms, the fibers away from the neutral axis are subjected to tension and compression. The fibers under compression heat slightly, while those under tension cool slightly. This creates a thermal gradient, which induces the flow of heat from the hot fibers to the cold fibers. Because of material properties, the beam does not reach thermal equilibrium instantaneously. This time lag is the direct cause of damping.

Since the aim is to increase the damping of a structure, a question that one might ask is "What happens if heat is applied externally to the structure?" In this paper we shall theoretically and experimentally show that when properly applied, such heating can be used to increase the material damping of a given structure.

The idea of *static* thermal shape control has been considered by a number of authors, including a numerical study

by Haftka and Adelman.[4] In addition, Allen and Haisler[5] have numerically analyzed the self-heating of a vibrating space structure. Boley and Barber[6] considered the response of beams and plates to rapid heating, but their results were of the "open loop" type. The author was unable to find any work on the topics of applied heating for *dynamical* control or experimental work relating to control by applied thermal gradients. This paper will deal with those issues.

As an example, we shall consider a cantilevered beam in free bending vibration. It will be assumed that the beam is equipped with some type of actuator that can produce a thermal gradient across the beam's section. The deformation under thermal loading will be calculated and coupled with the beam's elastic behavior. A control system will be designed to "close the loop" in order to increase the system's damping. Then, results of an experimental investigation on a beam structure will be presented.

In this analysis, repeated use of the Laplace transform will be made. It is an extremely powerful method for transient analysis and control system studies, both of which are present in this paper. If the variables are not labeled as time or frequency domain type, their type will be obvious from the context of the expression.

II. Analysis of Thermal Dynamics of Actuators

We shall consider the cross section of the beam as is shown in Fig. 1. It consists of two rectangular caps parallel to the x-y plane whose centroids are separated by a distance $2d$. The reason for the separation of the two caps is to provide space for the thermal actuators, which will be used to generate a thermal gradient vertically across the two caps of the beam. We will assume that the section of beam cap under consideration has a single thermal actuator in contact with it. The cap has specific heat capacity c.

If we assume two-dimensional geometry, that the top of the cap is insulated, and that the amount of heat flow Q is applied as a step input to the area S of its lower surface, it may be found[7] that the temperature distribution within the cap is (assuming null initial temperature)

$$T_{\text{step}} = \frac{Qt}{\rho chS} + \frac{Qh}{KS}\left[\frac{3\hat{z}^2 - h^2}{6h^2} - \frac{2}{\pi^2}\sum_{n=1}^{\infty}\frac{(-1)^n}{n^2}\exp\left(-\frac{\kappa n^2\pi^2 t}{h^2}\right)\cos\frac{n\pi\hat{z}}{h}\right] \tag{1}$$

where T_{step} is the temperature perturbation (e.g., $T_{\text{step}} \equiv T_{\text{actual}} - T_{\text{ref}}$). To determine a transfer function, the *impulse response* is needed. The impulse response may be found from taking the time derivative of the step response (for simplicity, the definitions $\beta_n = \kappa n^2\pi^2/h^2$ and $\kappa = K/\rho c$ were used):

$$T \equiv \frac{\partial T_{\text{step}}(t)}{\partial t} = \frac{Q}{\rho chS}\left[1 + \frac{2}{\pi^2}\sum_{n=1}^{\infty}\frac{(-1)^n}{n^2}e^{-\beta_n t}\cos\frac{n\pi\hat{z}}{h}\right] \tag{2}$$

We will assume that the thermal actuators are voltage driven, and that they have a linear behavior in converting voltage to heat flow. We will define their conversion behavior as

$$Q(s) = C_{QV}\cdot V(s) \tag{3}$$

where C_{QV} is the assumed voltage to heat flow conversion constant, and $V(s)$ the Laplace transform of the voltage applied to a single actuator. In the experiment, the actuators are placed in series, so we define

$$V(s) = V_c(s)/n_s \tag{4}$$

where V_c is the voltage applied to all the actuators, and n_s the number of actuators in series.

When Eqs. (2-4) are combined, we obtain the expression relating temperature to voltage as

$$\frac{T(t)}{V_c(t)} = \frac{C_{QV}}{\rho chn_s S}\left[1 + \frac{2}{\pi^2}\sum_{n=1}^{\infty}\frac{(-1)^n}{n^2}e^{-\beta_n t}\cos\frac{n\pi\hat{z}}{h}\right] \tag{5}$$

This relation will be used to compute the thermal bending moment generated by the thermal actuators in Sec. III.

III. Thermal Bending Moment Calculation

We have assumed in the previous section that the temperature in the beam in the vicinity of a given actuator was constant (lumped mass approximation). The strain due to the temperature is αT, where α is the coefficient of thermal expansion of the beam cap. With these definitions, the thermal bending moment M_T may be calculated from

$$M_T(t) = \int\int_A E\alpha T(z,t)z\,dA \tag{6}$$

where E is Young's modulus, z the distance from the beam neutral axis, and A the total cap cross-sectional area. If we factor out the geometry-independent terms, we get

$$M_T(t) = 2E\alpha\int\int_{\substack{A\\ \text{one cap}}} T(z,t)z\,dA \tag{7}$$

Here we have assumed temperature independent material properties and symmetry, which gives a factor of two to account for both caps. We may evaluate the width integral separately

$$\int\int_{\substack{A\\ \text{one cap}}} z\,dA = \int_0^b dy\int_{z=d-\frac{1}{2}}^{d+\frac{1}{2}} T(z)z\,dz = b\int_{z=d-\frac{1}{2}}^{d+\frac{1}{2}} T(z)z\,dz \tag{8}$$

where we have used $\int_0^b dy = b$ to obtain the last result.

To evaluate the remaining integral, we require the function $\hat{z}(z)$. From geometry, $\hat{z} = -z + d + h/2$. After some algebra and change of variables, we find that

$$\frac{M_T(t)}{V_c(t)} = \frac{2\alpha bC_{QV}dE}{\rho chn_s S}\left[1 - \frac{4}{\pi^2}\frac{h}{d}\sum_{n=1,3,5,\ldots}^{\infty}\frac{e^{-\beta_n t}}{n^2}\right] \tag{9}$$

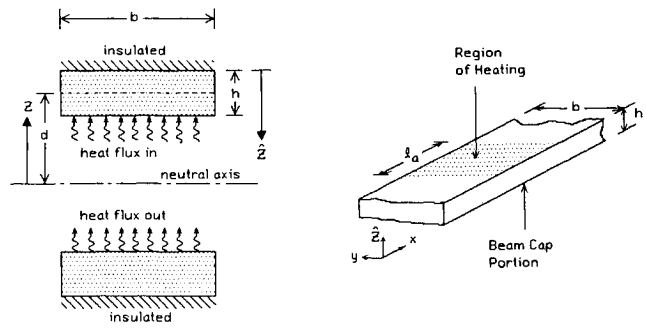

Fig. 1 Details of the thermoelectric beam. The left-hand figure is the beam cross section; the right-hand illustration shows the side view geometry.

The Laplace transform of Eq. (9) is found to be

$$\frac{M_T(s)}{V_c(s)}=\frac{2\alpha bC_{QV}dE}{\rho chn_sS}\left(\frac{1}{s}-\frac{4}{\pi^2}\frac{h}{d}\sum_{n=1,3,5,\ldots}^{\infty}\frac{1/n^2}{s+\kappa n^2\pi^2/h^2}\right) \tag{10}$$

where we have used $\mathcal{L}\{1\}=1/s$ and $\mathcal{L}\{e^{-\alpha t}\}=1/(s+\alpha)$. [It will later be shown that the second term in parentheses in Eq. (10) may be neglected for the present analysis.]

IV. Dynamic Analysis of Beam under Thermal Loading

The geometry for the beam is shown in Fig. 2. We will use x for the spanwise variable and $w(x)$ for the beam deflection. The stations x_1 and x_2 represent the inner and outer locations of the distributed thermal actuator, a portion of which was examined in the previous section. x_s is the location of a sensor to be used for feedback control.

Rather than repeat an involved calculation, the equation of motion for the beam may be found in the text of Boley and Weiner,[8] which uses the Bernoulli-Euler description. This formulation is conventional, with the exception of the imposition of an *internally generated* distributed bending moment. We have already shown that our thermal actuators produce such a moment, so the referenced analysis is indeed applicable.

We present the equation of motion for our beam as

$$m(x)\frac{\partial^2 w(x,t)}{\partial t^2}+\frac{\partial^2}{\partial x^2}\left[EI(x)\frac{\partial^2 w(x,t)}{\partial x^2}\right]=\frac{\partial^2 M_T(x,t)}{\partial x^2} \tag{11}$$

where $M_T(x,t)$ is the *thermally induced* distributed bending moment applied to the beam. In the case considered here, the magnitude of M_T is constant, and it is assumed to begin at the location $x=x_1$ and end at $x=x_2$. Thus we may write

$$M_T(x,t)=M_T(t)\,[H(x_1)-H(x_2)] \tag{12}$$

where $H(x)$ is the Heaviside step function.

We now do a conventional expansion into normal modes, e.g.,

$$w(x,t)\equiv\sum_{n=1}^{\infty}\varphi_n(x)\cdot\xi_n(t) \tag{13}$$

We will assume that the $\varphi_n(x)$ are the mass-normalized mode shapes

$$\int_0^{\ell}\varphi_m(x)m(x)\varphi_n(x)dx\equiv\delta_{mn} \tag{14}$$

Then we may expand out Eq. (11) in the normal fashion

$$\int_0^{\ell}\varphi_m(x)m(x)\frac{\partial^2}{\partial t^2}[\varphi_n(x)\xi_n(t)]\,dx+\int_0^{\ell}\varphi_m(x)\frac{\partial^2}{\partial x^2}\left\{EI(x)\frac{\partial^2}{\partial x^2}[\varphi_n(x)\xi_n(t)]\right\}dx=\int_0^{\ell}\varphi_m(x)M_T(t)\frac{\partial}{\partial x}[\delta(x-x_1)-\delta(x-x_2)]\,dx \tag{15}$$

Here we have assumed that $H'(x)=\delta(x)$. After several integrations by parts, some simplifying, and using the definition of simple harmonic motion

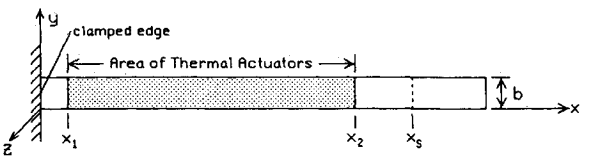

Fig. 2 Overall dimensions and layout of thermoelectric beam experimental apparatus.

$$\int_0^{\ell}\varphi_m(x)\frac{\partial^2}{\partial x^2}\left[EI\frac{\partial^2}{\partial x^2}\varphi_m(x)\right]dx\equiv\omega_m^2 \tag{16}$$

we get

$$\xi_m''(t)+\omega_m^2\xi_m(t)=M_T(t)\int_0^{\ell}\varphi_m(x)\,[\delta'(x-x_1)-\delta'(x-x_2)]\,dx \tag{17}$$

We have written the derivative of a delta function as $\delta'(x)$. The expression may be simplified further by using the result[9] $\int_a^b\delta'(u-t_1)f(u)du=-f'(t_1)$ for $a<t_1<b$. Then we have as the beam equation

$$\xi_m''(t)+\omega_m^2\xi_m(t)=M_T(t)\,[\varphi_m'(x_2)-\varphi_m'(x_1)] \tag{18}$$

To make this relation more useful to the present experiment, we will make the following changes: First, we will assume that only the first mode is of importance. Second, we will modify the equation empirically to include the presence of modal damping. Rather than retain the subscript 1 (for the first mode), we will write $\varphi(x)$ as the mode shape. Thus, we have the simplified system equation

$$\xi''(t)+2\zeta\omega\xi'(t)+\omega^2\xi(t)=M_T(t)\,[\varphi'(x_2)-\varphi'(x_1)] \tag{19}$$

To facilitate the analysis of Eq. (19), we take its Laplace transform

$$(s^2+2\zeta\omega s+\omega^2)\xi(s)=M_T(s)\,[\varphi'(x_2)-\varphi'(x_1)] \tag{20}$$

V. Sensor Dynamics

To consider the control system as an integrated part of the system, we must consider the dynamics of the sensor and the actuator. The dynamics of the actuator have already been described (Secs. II and III), so we will only consider the sensor here.

Strain gages, optical sensors, and many other types of sensors may be employed for motion sensing, however, we chose to use an accelerometer because of availability. The accelerometer produces a signal proportional to the acceleration that it experiences, e.g.,

$$V_s=G_s\frac{\partial^2 w(x_s)}{\partial t^2} \tag{21}$$

where V_s is the voltage produced by the accelerometer, and G_s is the proportionality constant (volts/unit acceleration). Since we have assumed harmonic motion, the above equation is replaced by

$$V_s(s)=-G_s\omega^2 w(x_s)=G_s\omega^2\xi(s)\varphi(x_s) \tag{22}$$

Hence, the transfer function for the sensor is

$$\frac{V_s(s)}{\xi(s)}=-G_s\omega^2\varphi(x_s) \tag{23}$$

We will now consider the details of "closing the loop" and a control system.

VI. Control System Analysis

We now must consider the contribution of the mode shape $\varphi(x)$ to this problem. Although it is possible to calculate analytically the mode shape, it is more convenient to solve this problem numerically. For this particular problem, the finite element code NASTRAN was employed to provide mass-normalized mode shapes. When the computed values of $\varphi'(x_2)$ and $\varphi'(x_1)$ are input into Eq. (20), we have the following system equation (numerical values for the parameters in all the equations are given in the Appendix)

$$(s^2+2\zeta\omega s+\omega^2)\xi(s)=1.583M_T(s) \tag{24}$$

Equation (10) becomes

$$\frac{M_T(s)}{V_c(s)}=8.49\times10^{-3}\ \frac{\text{N}\cdot\text{m}}{\text{volt}\cdot\text{sec}}\left[\frac{1}{s}-\left(\frac{1.473}{s+1171}+\cdots\right)\right] \tag{25}$$

The first term in parentheses on the right-hand side of Eq. (25) has a time constant far faster than the open loop time constant of the thermal actuators (approximately 15 rad/s) and may thus be discarded, along with all of the other terms in the infinite series in Eq. (10). (The remaining part, $1/s$, represents the "lumped mass" approximation of the thermal response.) Accordingly, the system equation becomes

$$\frac{\xi(s)}{V_c(s)}=\frac{0.01344}{s(s^2+0.222s+183.2)} \tag{26}$$

The accelerometer has a gain $G_s=0.491$ volts/g. Including the system's natural frequency of 2.154 Hz, the sensor transfer function is found to be

$$\frac{V_s(s)}{\xi(s)}=7.151\ \frac{\text{volts}}{\text{modal displacement}} \tag{27}$$

We now have all the ingredients necessary to "close the loop" except that the system will likely need some sort of compensation for stability. We shall later define it explicitly, but for now, we represent the compensation dynamics as $C(s)$.

To determine the necessary compensation, we consider the *open loop* transfer function for the modal displacement $\xi(s)$ to the control voltage V_c, which is the product of Eqs. (26) and (27)

$$\frac{\xi(s)}{V_c(s)}=\frac{0.0961}{s(s^2+0.222s+183.2)} \tag{28}$$

This transfer function has a pole at the origin (from the integrator-type behavior of the thermal mass) and a pair of complex conjugate poles very close to the imaginary axis (from the first vibrational mode of the beam). From the rules of plotting roots loci, this system will be unstable with either positive or negative proportional feedback, as either will cause the closed-loop poles to migrate into the right-half plane. A higher order compensation scheme is necessary.

With simple lead compensation, we can move the loci centroid into the left-hand plane, but analysis shows that two cascaded lead compensators will be more effective. The transfer function for the two cascaded lead compensators is represented by

$$C(s)=K_c\frac{(s+a)^2}{(s+b)^2} \tag{29}$$

where the poles are located at $-b$ on the real axis and the zeros are located at $-a$ on the real axis, and K_c is the (as yet unspecified) gain of the compensation, which may be adjusted for better closed-loop performance. When a and b of the lead compensators are chosen to be located at 5 and 55 rad/s, respectively, the compensator's overall transfer function is found to be

$$K_c\frac{(s+5)^2}{(s+55)^2} \tag{30}$$

Combining the compensation transfer function (30) with the system equation (28), we have the following transfer function:

$$\frac{\xi(s)}{V_c(s)}=K_c\frac{0.0961(s+5)^2}{s(s^2+0.222s+183.2)(s+55)^2} \tag{31}$$

The closed-loop system diagram for Eq. (31) is shown in Fig. 3.

A root locus diagram with such compensation is shown in Fig. 4. One can see that the loci all move into the left-half plane as the compensator gain increases. This results in a stable system, with increased damping as desired. (It should be pointed out that no attempt was made to find the "optimal" compensation; however, the control law used here was successful in increasing system damping.)

VII. Experimental Investigation

An apparatus was constructed to investigate experimentally the behavior of the coupled beam/actuator system. It consisted of a layered beam assembled from two aluminum caps on either side of a number of thermoelectric heat pumps. The two caps were machined from 2024-T3 aluminum and assembled with a number of screws. The caps were designed so that the thermoelectric modules would be a press fit between them, which would tend to minimize the damping in the structure caused by sliding between the two caps. Only the material damping of the caps themselves would remain. After the beam was assembled, it was securely clamped into a heavy vise, as an approximation of a cantilever beam. Lead wires were connected to the thermoelectric actuators, which were wired in five groups of three in series. The wires were tied down regularly along the beam so that there was little possibility of the wires contributing to the damping. A photograph of the beam is shown in Fig. 5.

In order to reduce the frequency of the cantilever beam, a concentrated mass was attached to the tip of the beam. This mass (which is not shown in any of the figures) was supported vertically by a long, flexible wire. The purpose of this

Table 1 Performance summary

Description	Damping ratio ζ, %	Frequency, Hz
Open loop (measured)	0.81	2.15
Closed loop (calculated)[a]	9.2	2.66
Closed loop (measured)[a]	7.4	2.08

[a] Gain = 2050.

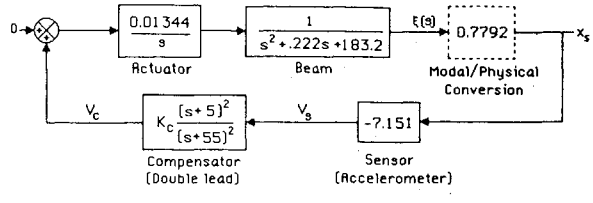

Fig. 3 Closed loop system diagram.

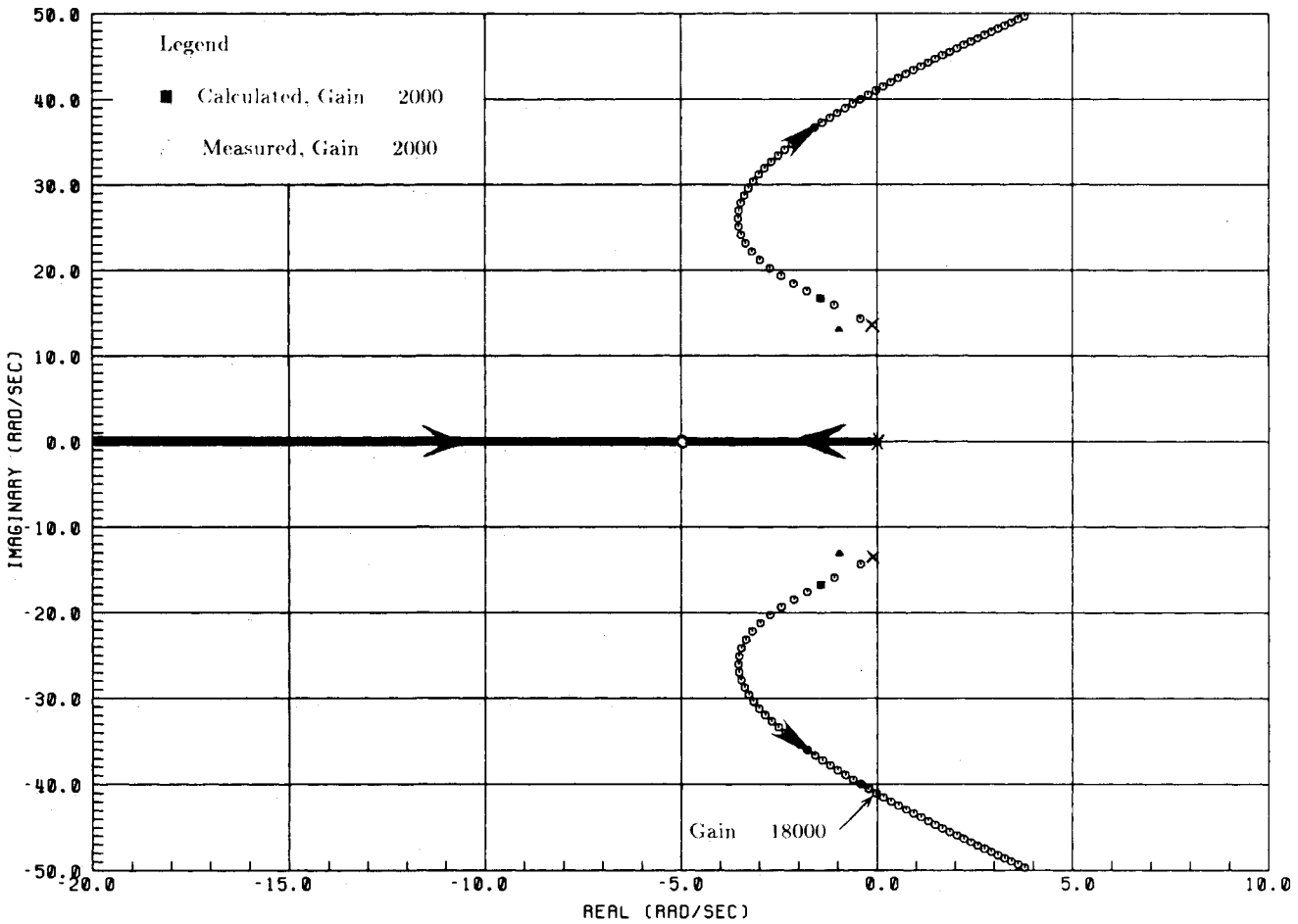

Fig. 4 Root locus of thermoelectric actuator/beam system combined with double lead compensation.

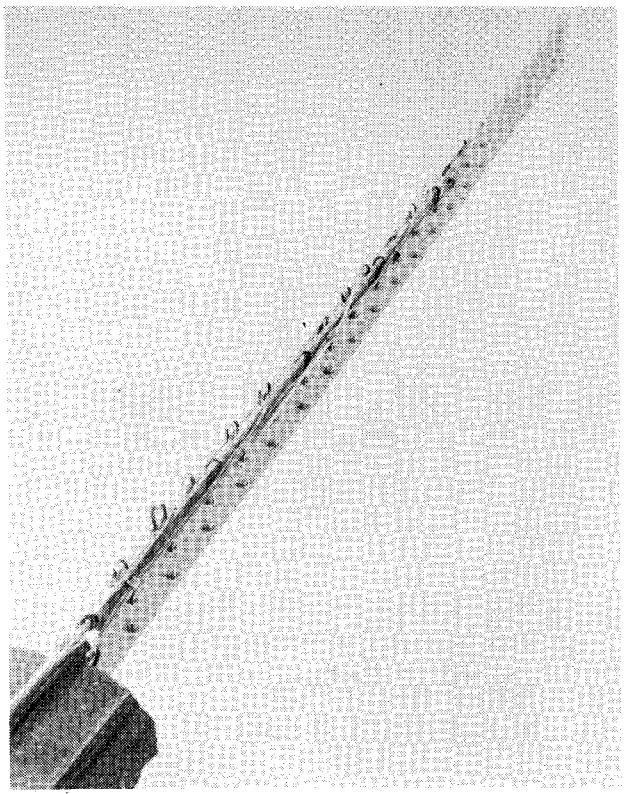

Fig. 5 Photograph of the beam used in the experiment.

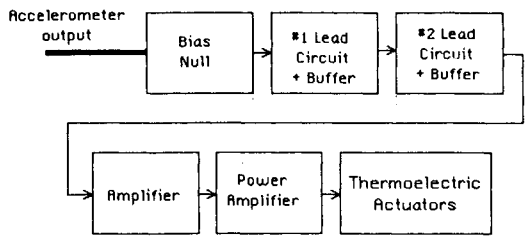

Fig. 6 Block diagram of the compensation circuit used for the experiment.

wire was to unload the beam assembly and to prevent the mass from causing lateral buckling. The tip mass also provided a convenient location for the mounting of an accelerometer, whose signal was fed back to the actuators for the closed loop system. The accelerometer cable was also secured to the beam to prevent any contribution to the system's damping.

The thermoelectric modules had very low electrical impedence so a high-current amplifier was needed. A set of such were constructed using high-current integrated-circuit operational amplifiers. A custom printed-circuit board was designed, and five amplifiers were fabricated, one for each set of three actuators. The amplifiers had provisions for limiting current output and adjustable gain setting, although the amplifiers had unity gain throughout the work reported.

A plug-in type circuit board was used to construct the electronics necessary for signal amplification and the double lead

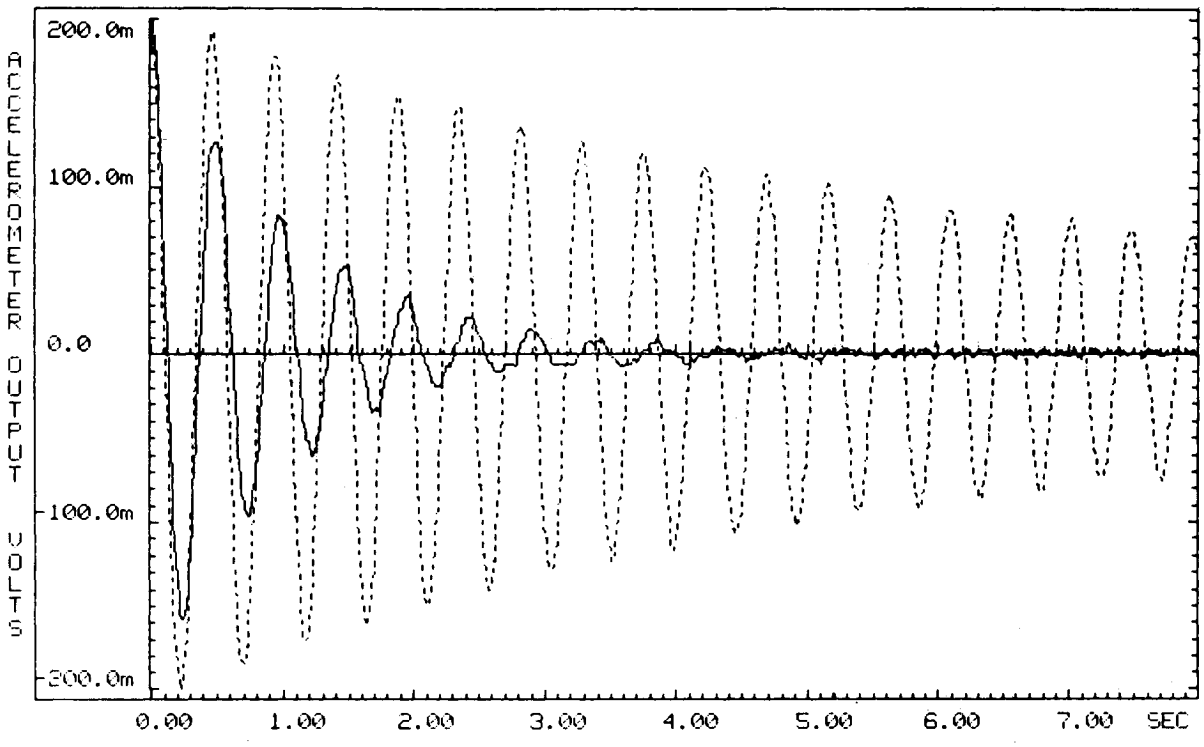

Fig. 7 Open- and closed-loop decay of system (solid = closed loop, dashed = open loop). Numerical results are given in Table 1.

compensators. This board had provisions for nulling the output, increasing the amplitude of the signal, and changing the time constants of the lead networks. The lead compensators were created by networks of resistors and capacitors, details of which may be found in an analog filter textbook such as Sage.[10] Buffer circuitry was used to eliminate loading effects between the two stages of compensation, as well as to buffer the output from the accelerometer electronics. A block diagram of the electronic setup is shown in Fig. 6.

With the control system turned off, the tip of the beam was deflected and then released, which resulted in the free sinusoidal decay shown by dashed lines in Fig. 7. With K_c chosen to be approximately 2050, the system was energized, and the tip of the beam was again deflected and released. This resulted in the decay shown in solid lines in the figure. It can clearly be seen that the settling time has been greatly reduced with the addition of the control system. Table 1 gives the open and closed loop data for the experiment.

VIII. Discussion of Results

A comparison of the experimental results with the performance predicted by the root locus (Fig. 4) reveals several discrepancies. First, the frequencies associated with the root location predicted by using the gain of 2050 in the closed loop system does not coincide with that obtained by the transient testing given above. In addition, the *behavior* of the closed loop system is qualitatively different. The root locus diagram predicts that as the gain is increased, the frequency of the system will increase. But the experimental results indicate a *decrease* in frequency. These discrepancies are probably due to the simplistic nature of the theoretical analysis and the number of simplifying assumptions that were made.

For example, the Bernoulli-Euler beam model could be replaced by a higher-order Timoshenko beam formulation. The thermal analysis neglected spanwise conduction at the end of the actuators (x_1 and x_2) as well as through the beam section (which might be caused by the fasteners used to assemble the beam and the thermal conductivity of the thermoelectrics themselves). The insulated boundary conditions assumed at the outer faces of the beam would be modeled more realistically as convective boundaries. Radiation is also ignored, but since the temperature perturbations are in the tens of degrees about room temperature, this is probably a reasonable assumption. Finally, the assumed linear behavior of the thermoelectric elements may not be realistic for this application. All of these assumptions may have contributed to the discrepancies noted above.

There are other problems associated with the thermoelectric modules. Because they are real devices, they have losses which have not previously been accounted for. For example, in addition to the Peltier effect (which causes heat flow in the thermoelectrics when voltage is applied), there is the effect of Joule heating, i.e., i^2R heating, which occurs *whenever* there is current flow through the device. This is a one-way effect, so that whenever there is current flow, the temperature of the beam and actuators rises. The only mechanisms that will reduce the system's temperature are conduction, convection, and radiation. All of these are present in the laboratory, but only radiation is available to orbiting structures. More study is necessary to determine whether this thermal "saturation" process is likely to cause problems in the implementation of this idea in orbiting large space structures. It did cause difficulties during test, which required limited testing durations interspersed with cooling periods.

IX. Conclusions

We have shown in this paper that the idea of thermal actuators is both theoretically and experimentally feasible. Simple thermal, elastic, and control theory were successful in approximately predicting the performance of the system. For the case of a "plucking" input, the system's settling time was decreased by an order of magnitude. Problems with the time lag due to thermal heat flow were shown to be unimportant in the closed loop system, which could successfully respond to signals greater than 2 Hz in frequency.

Appendix—Values of Physical Parameters

The following numerical values were used in the equations:

$b = 0.0381$ m	$x_1 = 0.0163$ m
$C_{QV} = 3.45$ W/V	$x_2 = 0.451$ m
$c = 963$ m^2/s^2 K	$x_s = 0.606$ m
$d = 7.11 \times 10^{-4}$ m	$\alpha = 2.43 \times 10^{-5}$/K
$E = 73.1$ GPa	$\zeta = 0.081$, measured open loop
$G_s = 0.491$ V/g	$\kappa = 6 \times 10^{-5}$ m^2/s
$h = 1.956 \times 10^{-4}$ m	$\omega = 13.53$ rad/s, open loop
$K = 156$ kg m s^3/K	$\rho = 2700$ kg/m^3 (aluminum)
$\ell = 0.606$ m	$\varphi'(x_1) = 0.0945$
$\ell_a = 0.0362$ m	$\varphi'(x_2) = 1.677$
$n_s = 3$	$\varphi(x_s) = 0.7792$

Acknowledgments

This research was carried out at Jet Propulsion Laboratory, California Institute of Technology, under a contract with the National Aeronautics and Space Administration Office of Aeronautics and Space Technology. The author would like to thank Caltech research assistant and Ph.D. candidate James Fanson for many enlightening and valuable discussions concerning the derivation of modal system equations, the implementation of closed loop control both theoretically and with hardware, and for suggestions regarding this paper. The author would also like to express his thanks to Professor Holt Ashley of Stanford University, whose discussions of passive damping during the author's research assistantship sparked the present work.

References

[1]Zener, C. M., *Elasticity and Anelasticity of Metals*, Univ. of Chicago Press, Chicago, 1948.

[2]Ashley, H., "On Passive Damping Mechanisms in Large Space Structures," *Journal of Spacecraft and Rockets*, Vol. 21, Sept.-Oct. 1984, pp. 448-455.

[3]Lee, U., "Thermoelastic and Electromagnetic Damping Analysis," *AIAA Journal*, Vol. 23, Nov. 1985, pp. 1783-1790.

[4]Haftka, R. T. and Adelman, H. M., "An Analytical Investigation of Shape Control of Large Space Structures by Applied Temperatures," *AIAA Journal*, Vol. 23, March 1985, pp. 450-457.

[5]Allen, D. H. and Haisler, W. E., "Predicted Temperature Field in a Thermomechanically Heated Viscoplastic Space Truss Structure," *Journal of Spacecraft and Rockets*, Vol. 23, March-April 1986, pp. 178-183.

[6]Boley, B. A. and Barber, A. D., "Dynamic Response of Beams and Plates to Rapid Heating," *Journal of Applied Mechanics*, Vol. 24, Sept. 1957, pp. 413-416.

[7]Carslaw, H. S. and Jaeger, J. C., *Conduction of Heat in Solids*, Oxford Univ. Press, Oxford, 1959, p. 112.

[8]Boley, B. A. and Weiner, J. H., *Theory of Thermal Stresses*, John Wiley & Sons, New York, 1960, p. 338.

[9]Hildebrand, F. B., *Advanced Calculus for Applications*, 2nd ed., Prentice-Hall, Englewood Cliffs, NJ, 1976, p. 86.

[10]Sage, A. P., *Linear Systems Control*, Matrix Publishers, Inc., Champaign, IL, 1978, p. 81.